Towards Detailed Cortical Maps of the Human Back with Representational Similarity Analysis

Authors: Alexandros Guekos[1,2], David M Cole[1,3], Monika Dörig[4], Philipp Stämpfli[3,5], Louis Schibli[6], Philipp Schuetz[6], Michael L Meier[1]

Institution:

[1] Integrative Spinal Research, Department of Chiropractic Medicine, Balgrist University Hospital, University of Zurich, Zurich, Switzerland

[2] Decision Neuroscience Lab, Institute of Human Movement Sciences and Sport, Department of Health Sciences and Technology, ETH Zurich, Zurich, Switzerland

[3] Department of Psychiatry, Psychotherapy and Psychosomatics, Psychiatric University Hospital, University of Zurich, Switzerland

[4] School of Engineering and Architecture, Lucerne University of Applied Sciences and Arts, Horw, Switzerland

[5] MR-Center of the Psychiatric University Hospital, Department of Child and Adolescent Psychiatry, University of Zurich, Zurich, Switzerland

[6] Competence Center Thermal Energy Storage, Lucerne University of Applied Sciences and Art, Horw, Switzerland

Corresponding author: Alexandros Guekos, Integrative Spinal Research, Balgrist Campus, Lenghalde 5, 8008 Zurich, Switzerland, alexandros.guekos@balgrist.ch

Abstract

Background

Cortical reorganization and its potential pathological significance is increasingly studied in chronic low back pain (CLBP) patients. Yet, detailed cortical maps of the healthy human back are lacking. To better understand cortical changes during the development and maintenance of CLBP, a detailed baseline characterization resulting from sensory thoracolumbar afferent input is needed. To this end, a novel pneumatic vibrotactile stimulation method was used to stimulate paraspinal sensory afferents while studying their cortical representations in unprecedented detail.

Methods

In 30 young healthy participants, vibrotactile stimulations at 20Hz and 80Hz were applied bilaterally at nine locations along the thoracolumbar axis while functional magnetic resonance imaging (fMRI) was performed. A whole-brain searchlight representational similarity analysis (RSA) in combination with different experimental models of paraspinal afferent input was used to investigate the representational organization of the respective neuronal activation patterns.

Results

For 80Hz, the organizational structure of the neuronal activation patterns yielded the best fit for a model based on segmental distances between the stimulated paraspinal locations, located bilaterally in the primary (S1) and secondary somatosensory (S2) cortices. For 20Hz, this observation was restricted to the right S1.

Conclusions

fMRI during paraspinal vibrotactile stimulation in combination with RSA is a powerful tool that can be used to establish highly detailed cortical maps of the human back. The current findings constitute a promising basis to further explore cortical reorganization and its potential pathological meaning in CLBP patients.

Funding

Primary funding (as part of a project grant to MLM): Swiss National Science Foundation, Bern, Switzerland (ID 320030 185123).

1. Introduction

Over the course of the adult life, the thoracolumbar regions of the human back, comprising the thoracic and lumbar segments of the spine, suffer the biomechanical and neuronal consequences of spinal changes, such as intervertebral disc degeneration, decrease in bone density, or alterations of trabecular morphology (Andersson, 1998, Benoist, 2005, Ferguson and Steffen, 2005). Such changes, to varying degrees, affect postural stability, movement flexibility, range of motion, and sensory perception along the thoracolumbar axis (Intolo et al., 2009, Saidu et al., 2011, Finsback and Mannerkorpi, 2005, Ferlinc et al., 2019, Kim et al., 2020). They are thought to contribute to the aetiology of back pain phenotypes in patient populations with and without clear underlying pathologies and can affect spinal and supraspinal systems (Papadakis et al., 2011, Koch and Hänsel, 2019, Pinto et al., 2020). With respect to supraspinal mechanisms, growing evidence suggests that chronic low back pain (CLBP) is linked to neuroplastic adaptations of the brain (Flor et al., 1997, Ung et al., 2014, Rodriguez-Raecke et al., 2014, Konno and Sekiguchi, 2018). Thus, in light of its potential clinical relevance, neural reorganization, specifically in the primary somatosensory and in the motor cortices, has been studied with growing interest in back pain contexts (Flor et al., 1997, Flor, 2003, Tsao et al., 2010, Van Dieën et al., 2017, Zhang et al., 2019, Jenkins et al., 2022, Moseley and Flor, 2012).

As of yet, however, it is difficult to position all of these findings at the cortical level within a coherent narrative, because only very little is known about the neural representations of the human back in general. Detailed cortical maps are lacking. In particular, there is no fine-grained mapping of the cortical representations of the sensory afferents of the healthy back along the thoracolumbar axis. Yet, such a baseline characterization of back representations, e.g., reflecting the neural state before any pain-related changes have even set in, seems crucial to understanding

the trajectory of neural reorganization processes accompanying the changes at the spinal level.

One promising way to establish a cortical topographic mapping of the healthy human back at such a baseline is by assessing neural representations of paraspinal sensory perception based on vibrotactile stimulation. Signal transduction from mechanical afferent input, such as vibration, follows the dorsal column-medial lemniscus pathway before being transmitted via the brainstem through the thalamus to the primary somatosensory and motor cortices (Kandel et al., 2013). To decipher the cortical responses to activation of mechanoreceptors in these and other cortical regions, vibrotactile stimulation at specific frequencies can be used (Harrington and Downs III, 2001, Gilman, 2002, Kim et al., 2015). Depending on the vibration frequency, different mechanoreceptors are activated, such as Meissner corpuscles at lower frequencies and deeper located Pacinian corpuscles or muscle spindles at higher frequencies (Avanzino et al., 2014, Weerakkody et al., 2007).

A novel method for studying the cortical activation patterns of paraspinal sensory stimulation along the thoracolumbar axis in a highly reproducible manner is the *pneumatic vibration device* (pneuVID), which applies vibrotactile stimuli to the back at specific frequencies and can be easily combined with functional magnetic resonance imaging (fMRI) data acquisition (Schibli et al., 2021). Paradigms using vibrotactile stimuli, which correspond to a naturalistic afferent input, are an established way of assessing cortical somatotopic representations from different body parts (Harrington and Downs III, 2001, Kim et al., 2016, Schellekens et al., 2021). The usefulness of pneuVID to assess the neural representations of the human back has recently been validated using univariate statistical neuroimaging techniques (Cole et al., 2022). Representations based on univariate analysis are a first step towards establishing the cortical mapping of the healthy human back. Yet, on their own, they are unqualified to provide a better understanding of the detailed organiza-

tional structure of functional representations, i.e., topographic information content. For instance, it remains open for investigation as to whether or not spatially distinct univariate functional representations of paraspinal sensory input imply detailed neural topographic information representing differential segmental afferent input along the thoracolumbar axis.

An up-and-coming tool that is designed to answer such questions is representational similarity analysis (RSA). As an analytical framework to both assess and relate measured neural activity to computational and behavioural models (Kriegeskorte et al., 2008a), RSA has been successfully implemented for multivoxel pattern analysis (Kriegeskorte et al., 2008b, Dimsdale-Zucker et al., 2018, Dimsdale-Zucker and Ranganath, 2018, Popal et al., 2019, Ejaz et al., 2015, Gooijers et al., 2022). The pattern information can be stored in a representational dissimilarity matrix (RDM), the cells of which quantify the dissimilarity in neural activation for every pair of experimental conditions (brain RDM). The brain RDM is then compared for correlation with the RDM of an explanatory model (model RDM) (Kriegeskorte et al., 2008a).

Using RSA, the present study aimed to reveal novel insights into the topographic organization of cortical activation patterns resulting from different paraspinal afferent inputs along the thoracolumbar axis. Brain RDMs were derived from neural activation following vibrotactile stimulations using pneuVID at two specific frequencies (20Hz and 80Hz). In order not to bias the results regarding cortical localization, a whole-brain searchlight analysis was performed (Kriegeskorte et al., 2006, Nili et al., 2014, Dimsdale-Zucker and Ranganath, 2018), aiming to determine which brain regions contain the highest levels of information content in line with multiple proposed model-based topographic organizational configurations of paraspinal afferents. The model RDMs were motivated by anatomical and biomechanical characteristics of the spine.

The best fitting model was hypothesized to uncover topographically informative activation patterns primarily located in the primary and secondary somatosensory cortices (S1, S2) and the motor cortex (M1), providing novel and detailed information about the cortical organization of the healthy human back.

2. Methods

2.1. General Study Design

The study followed a within-subject experimental design including one magnetic resonance imaging (MRI) session with vibrotactile stimulation of the back. Study approval was obtained from the ethics board of the Canton of Zurich. The study observed the principles of the Declaration of Helsinki.

2.2. Participants

All participants (N=30, 18 women) were healthy pain-free adults between 18 and 39 years of age (28.7 $\pm$ 5.5) and a body mass index below 30 kg/m^2 (22.2 $\pm$ 2.8). Exclusion criteria were the presence of any acute or recurrent back pain within the past three months, any history of chronic pain, prior spine, foot, or ankle surgery, any history of psychiatric or neurological disorders, excessive consumption of alcohol, other intoxicants, or analgesics within the past 24 hours, neuromuscular diseases, impairments of the motor system, MRI contraindications, lateralization of sensory perception along the thoracolumbar axis, or inability to distinguish the sensations evoked by the two stimulation frequencies from one another.

2.3. Testing Procedure

2.3.1. Participant Setup

Nine spinous processes, $T3$, $T5$, $T7$, $T9$, $T11$, $L1$, $L3$, $L5$, and $S1$ (T=thoracic, L=lumbar, S=sacral), were manually identified on the back of every participant by an experienced physiotherapist for subsequent attachment of the pneuVID units. For the duration of the experiment, participants were lying in a supine position on the bed of the MRI scanner with their eyes open.

2.3.2. Pneumatic Vibration Device (pneuVID)

Full details on the pneuVID methodology and its integration into the MRI environment have previously been outlined (Schibli et al., 2021, Cole et al., 2022). In short: vibrotactile stimulation units are attached bilaterally to the identified spinous processes; a valve box delivers pulses of compressed air to the vibrational units; and a control module (Raspberry Pi, Cambridge, UK) connects the setup to the MRI system.

In the present study, the units vibrated bilaterally at one of the nine locations at 20Hz or 80Hz with amplitudes of 0.5 to 1 mm for a stimulus duration of five seconds. Two stimulation runs were performed with 6 stimuli per back location and frequency, i.e., a total of 108 stimuli per run ($2 \cdot 6 \cdot 9 = 108$). The interstimulus interval randomly varied from 4 to 7 seconds. The stimulation order was pseudo-randomized between participants with the restriction of a maximum of three consecutive stimuli at the same location or frequency. The air pressure of the delivered pulses was kept constant at 1.5bar during the experiment.

The two stimulation frequencies of 20Hz and 80Hz were chosen because they are thought to activate different tactile and proprioceptive afferents of superficial and deep mechanoreceptors (Roll and Vedel, 1982, Avanzino et al., 2014, Schellekens et al., 2021). Meissner corpuscles should be activated by 20Hz while 80Hz has been shown to be a potent stimulus for activating muscle spindles, which are supposed to be the primary proprioceptors in the human body (Proske and Gandevia, 2012). However, it should be noted that these frequency-mechanoreceptor relationships are not exclusive as Pacinian corpuscles may also be co-stimulated during 80Hz stimulation (bandwidth between 80-400 Hz) and have been shown to transmit proprioceptive information through skin stretch (Weerakkody et al., 2007, LaMotte and Mountcastle, 1975, Talbot et al., 1968).

2.3.3. Neuroimaging Data Acquisition

Data acquisition was performed on a Philips Achieva 3T MRI scanner with a head coil of 32 channels (Philips, Best, The Netherlands). Both stimulation runs lasted 22.5 minutes. Per run, 750 volumes of echo-planar imaging (EPI) were acquired with T2*-weighting (TR=1.8s; TE=34ms; flip angle=70°; 54 interleaved ascending axial slices with multiband factor 3; in-plane resolution=1.72·1.72mm^2; slice thickness=2.0mm with no slice gap; sensitivity encoding factor=1.4; EPI factor=87). Between the two runs, a T1-weighted anatomical scan was acquired (sequence=MPRAGE; TR=6.6ms; TE=3.1ms; flip angle=9°; field of view=230·226·274; voxel size=1.0·1.0·1.2mm^3; turbo field echo factor=203).

2.4. Representational Similarity Analysis (RSA)

The Python Representational Similarity Analysis toolbox (rsatoolbox v.0.0.4) (Kriegeskorte et al., 2021) was used to implement RSA. It was carried out on Jupyter Notebooks v1.0.0 (Jupyter, 2021) with Python v3.8.10 (Python Software Foundation, Delaware, USA) and NiBabel v3.2.2 (Brett et al., 2022), Nilearn v0.9.0 (Abraham et al., 2014), NLTools v0.4.5 (Chang et al., 2021), Pandas v1.4.1 (McKinney and the Pandas Development Team, 2022), and Seaborn v0.11.2 (Waskom, 2021). RSA was run within a supercomputing environment (ScienceCloud, University of Zurich, Switzerland).

2.4.1. Data Pre-Processing

Pre-processing of acquired neuroimaging data followed a previously published pipeline (Cole et al., 2022).

For every participant, mean activation contrasts normalized to the MNI standard space (2mm isotropic voxels) were obtained for each of the nine conditions (corresponding to the nine paraspinal locations). This was done separately for the two stimulation frequencies, i.e. for 20Hz and 80Hz compared to baseline. Prior

to analysis, data were smoothed with a 4mm Gaussian kernel in order to compare the results on the group level (Kriegeskorte et al., 2006).

Two brain masks were created using an atlas-based probabilistic approach (as defined by the Juelich Histological Atlas (Geyer et al., 1996, 2000)). The M1 mask comprises Brodmann areas (BA) BA4a and BA4p and the S1 mask BA3a, BA3b, BA1, and BA2 as well as BA5 of the posterior parietal cortex. The choice of these two masks was motivated by the previously published results on neural processing of tactile and vibrotactile stimulation (Delhaye et al., 2018, Schellekens et al., 2021, Cole et al., 2022). The probabilistic atlas threshold was set at 20% causing some overlap between the two masks.

2.4.2. Searchlight Approach

In a RSA searchlight analysis, a small volume is moved over a pre-defined brain region (Dimsdale-Zucker and Ranganath, 2018). In the present study, a whole-brain spherical searchlight analysis was performed with a searchlight diameter of 5 voxels (Kriegeskorte et al., 2006, Etzel et al., 2013) including a total of 163,225 searchlights.

2.4.3. Representational Dissimilarity Matrices of Neural Activation (brain RDMs)

For every participant, a 9·9 brain RDM was created for each of the two contrasts. A RDM contains the dissimilarity information of neural activation patterns for every pair of experimental conditions, i.e. for every pair of stimulated paraspinal locations. By way of construction, every brain RDM is symmetrical with a diagonal of zeros regardless of the dissimilarity measure chosen. In the present study, the dissimilarity was quantified using the crossvalidated Mahalanobis distance (CMD) which gives an estimate of the geometrical distance between two activation patterns taking into account noise covariance and using data partitioning for crossvalidation (Kriegeskorte et al., 2006, Walther et al., 2016). CMD has been shown to be the most reliable dissimilarity measure for multivoxel pattern analysis (Walther et al.,

2016).

2.4.4. Model Representational Dissimilarity Matrices (model RDMs)

Figure 1 shows the schematics and the entries of the three experimental model RDMs that were used for RSA. The three models represent different degrees of complexity of thoracolumbar activation patterns with respect to their topographical structure.

First, the *simple model* is the most coarse approach. It only distinguishes between thoracic ($T3$-$T11$) and lumbosacral ($L1$-$S1$) regions. It mirrors the differences in anatomical characteristics of lumbosacral vertebrae on the one hand and higher located vertebrae on the other hand, such as larger bodies and facet joints with curved articular surfaces (Waxenbaum et al., 2017, Darby and Cramer, 2014). Neural activation patterns for the paraspinal afferents from the respective two regions therefore ought to reflect sensory inputs from the upper and lower back regions. As such, the *simple model* RDM contains zeros (i.e. total similarity) for pairs within the same and ones (i.e. total dissimilarity) for pairs within distinct regions.

Second, the *functional model* distinguishes upper thoracic ($T3$-$T7$), lower thoracolumbar ($T9$-$L1$) and lower lumbosacral ($L3$-$S1$) regions. This model RDM's entries are constructed the same way as for the *simple model*. The *functional model* represents the differences in spinal mobility in the three partitions. The upper thoracic region is the most rigid of the three, with true ribs and vertebral bodies orientated more ventrally with respect to the transversal plane. In contrast, the lower thoracolumbar segments with dorsally-inclined vertebral bodies, false ribs, and musculofascial integration into the lumbosacral region reflect a transition zone containing the thoracolumbar junction, i.e., the connection to the more mobile lumbosacral spinal region (Murphy et al., 2020, Park et al., 2016). The neural activation patterns of paraspinal afferent input should therefore reflect a tripartite organization of sensory inputs. Thus, the model RDM contains zeros for pairs within

the same region, 0.5 values for pairs of neighbouring regions, and ones for pairs of spatially separated regions (i.e. pairs of upper thoracic and lower lumbosacral regions).

Third, the *segmental model* reflects the organization of neural activation patterns which resemble human dermatome maps (Downs and Laporte, 2011). Paraspinal afferent input from neighbouring segments should result in more similar neural activation patterns than from segments located further apart, i.e., increasing anatomical distance should lead to higher dissimilarity in activation patterns. The dissimilarity entries in the *segmental model* RDM thus increase by 0.1 with distance (except for $L5$ to $S1$ which was set to 0.05 due to the comparatively shorter distance between these segments).

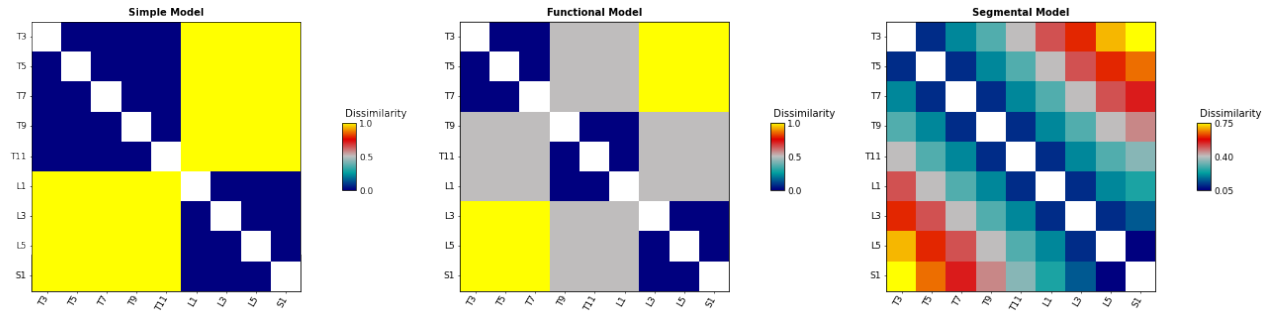

	T3	T5	T7	T9	T11	L1	L3	L5	S1
T3	0	0	0	0	0	1	1	1	1
T5	0	0	0	0	0	1	1	1	1
T7	0	0	0	0	0	1	1	1	1
T9	0	0	0	0	0	1	1	1	1
T11	0	0	0	0	0	1	1	1	1
L1	1	1	1	1	1	0	0	0	0
L3	1	1	1	1	1	0	0	0	0
L5	1	1	1	1	1	0	0	0	0
S1	1	1	1	1	1	0	0	0	0

	T3	T5	T7	T9	T11	L1	L3	L5	S1
T3	0.0	0.0	0.0	0.5	0.5	0.5	1.0	1.0	1.0
T5	0.0	0.0	0.0	0.5	0.5	0.5	1.0	1.0	1.0
T7	0.0	0.0	0.0	0.5	0.5	0.5	1.0	1.0	1.0
T9	0.5	0.5	0.5	0.0	0.0	0.0	0.5	0.5	0.5
T11	0.5	0.5	0.5	0.0	0.0	0.0	0.5	0.5	0.5
L1	0.5	0.5	0.5	0.0	0.0	0.0	0.5	0.5	0.5
L3	1.0	1.0	1.0	0.5	0.5	0.5	0.0	0.0	0.0
L5	1.0	1.0	1.0	0.5	0.5	0.5	0.0	0.0	0.0
S1	1.0	1.0	1.0	0.5	0.5	0.5	0.0	0.0	0.0

	T3	T5	T7	T9	T11	L1	L3	L5	S1
T3	0.00	0.10	0.20	0.30	0.40	0.50	0.60	0.70	0.75
T5	0.10	0.00	0.10	0.20	0.30	0.40	0.50	0.60	0.65
T7	0.20	0.10	0.00	0.10	0.20	0.30	0.40	0.50	0.55
T9	0.30	0.20	0.10	0.00	0.10	0.20	0.30	0.40	0.45
T11	0.40	0.30	0.20	0.10	0.00	0.10	0.20	0.30	0.35
L1	0.50	0.40	0.30	0.20	0.10	0.00	0.10	0.20	0.25
L3	0.60	0.50	0.40	0.30	0.20	0.10	0.00	0.10	0.15
L5	0.70	0.60	0.50	0.40	0.30	0.20	0.10	0.00	0.05
S1	0.75	0.65	0.55	0.45	0.35	0.25	0.15	0.05	0.00

Figure 1: Representational Dissimilarity Matrices for the three experimental models (model RDMs). Top row: Colour-coded schematics of the model RDMs (*simple model*, *functional model*, *segmental model*) with vertical bars indicating the dissimilarity colour scale (0=total similarity; 1=total dissimilarity). Bottom row: Numerical entries of the three model RDMs. Lines and columns are labelled according to the nine stimulated spinous processes $T3$-$S1$ (T=thoracic, L=lumbar, S=sacral).

2.5. Analysis

To compare brain RDMs to model RDMs, Kendall's rank correlation coefficient (Kendall, 1970) was used, because it is a robust measure when models are involved that predict tied ranks (Nili et al., 2014, Popal et al., 2019).

The correlation coefficients were first Fisher-z transformed (Walker, 2003). Then, a non-parametric permutation test with 5,000 iterations was performed which yielded an empirical distribution of null means. The p-value was obtained by the number of times the actual mean of the z-values exceeded the mean of the null distribution (from the permutations). The significance level was set at 0.001 (Stelzer et al., 2013, Wang et al., 2018).

A minimum threshold of 20 voxels was used to identify clusters of brain activity.

3. Results

Correlation analyses between brain RDMs and the three model RDMs were performed for both frequencies (20Hz and 80Hz). Figure 2 shows the results for the 5-voxels diameter before cluster thresholding. The p-values refer to the central node of the corresponding searchlight. For illustrative purposes, the masks for S1 and M1 were added to the figure.

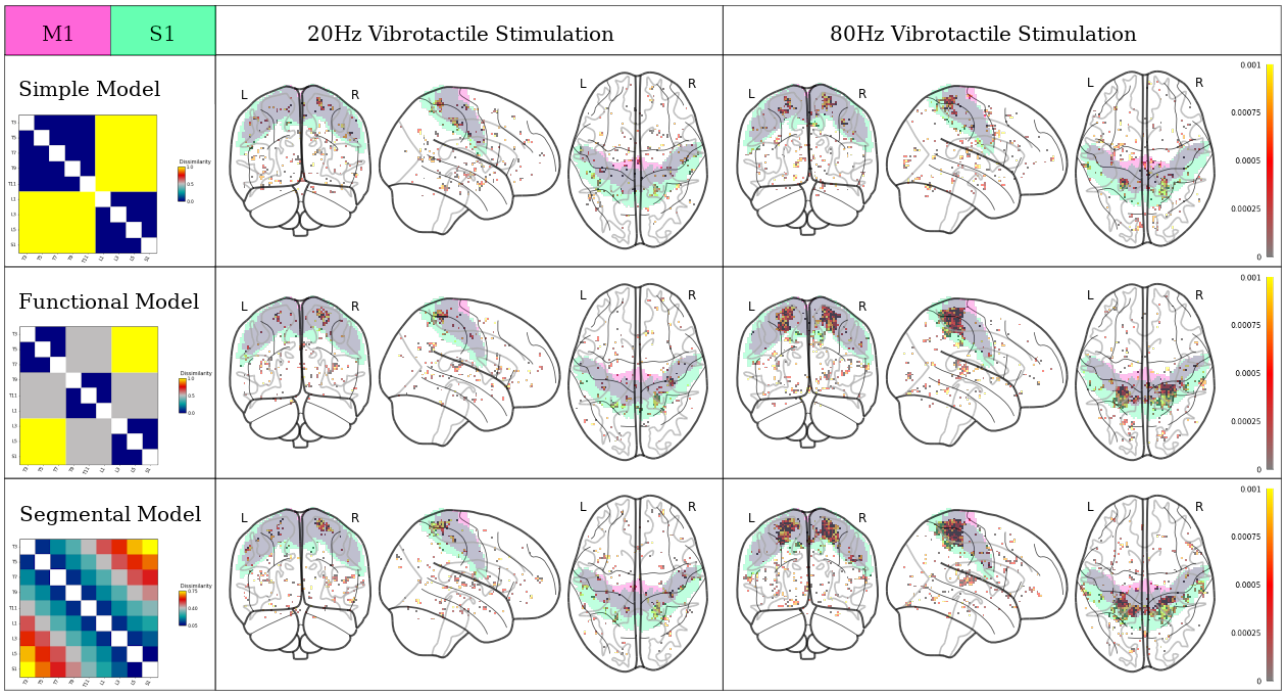

Figure 2: Significant correlations between the representational dissimilarity matrices of the neural activation (brain RDMs) and of the three experimental models (model RDMs) with respect to frequency of vibrotactile stimuli along the thoracolumbar axis for a 5-voxels diameter searchlight in coronal, sagittal, and axial view. Columns: vibrotactile stimulation frequencies of 20Hz and 80Hz. Rows: model RDMs (*simple model*, *functional model*, and *segmental model*) incl. colour-coded schematics and colour scales with lines and columns labelled according to the nine stimulated spinous processes $T3$-$S1$ (T=thoracic, L=lumbar, S=sacral). Colour coded p-values for correlations of the central node of the respective searchlight with colour scale from 0 to 0.001 (significance threshold). Masks for primary somatosensory (S1, green) and motor cortex (M1, magenta) with overlap (gray) are added to the views. M1 comprises Brodmann areas (BA) BA4a and BA4p and S1 BA3a, BA3b, BA1, and BA2 as well as BA5 of the posterior parietal cortex. The probabilistic atlas threshold was set at 20% causing some overlap between the two masks. L=left, R=right.

The whole-brain searchlight analysis yielded significant correlations between brain and model RDMs in several sensorimotor brain regions for all tested models (informative activation patterns, Figure 2). However, localization, and extent of the informative activation patterns were dependent on the tested model and frequency. For both stimulation frequencies (20Hz and 80Hz), a graduated improvement with respect to model performance can be visually identified, with the segmental model being the most informative model, in particular for 80Hz stimulation.

Figure 3 shows the informative activation patterns derived from the segmental model using a threshold of at least 20 voxels per cluster. For illustrative purposes, the best performing group-level brain RDMs for 20Hz and 80Hz are included. Detailed information on the respective clusters is summarized in Table 1.

For 20Hz, informative activation patterns were restricted to one cluster in the right hemisphere, primarily located within BA5 and to a lesser extent BA2.

For 80Hz, informative activation patterns were observed in two bilateral sets of regions. The first pair was localized within S1, mostly in BA2 and extending into BA3b, BA5, and BA7, the second one within S2 at the parietal operculum. For the first pair, the cluster on the right hemisphere extended into BA4p of M1.

Table 1: Cluster information for identified brain regions

Frequency (condition)	**Number of Voxels**	**Maximum significance** (p-value)	**COG X**	**COG Y**	**COG Z**	**Brain regions**
80Hz	488	<0.001	20	-42	60	R S1 BA2 & BA3b/SPL BA5/M1 BA4p
	434	<0.001	-22	-42	62	L SPL BA5 & 7/S1 BA2 & BA3b
	40	<0.001	*60*	-20	*10*	R S2, parietal operculum/STG
	35	<0.001	-8	-44	46	L SPL BA5
	34	<0.001	-62	-24	10	L S2, parietal operculum/STG
	20	<0.001	24	-46	50	R SPL BA7/S1 BA2
20Hz	76	<0.001	20	-44	66	R S1 BA2/SPL BA5

Cluster information for regions identified as significant by permutation testing of a 5-voxels diameter searchlight comparison of brain and *segmental model* representational dissimilarity matrices for 80Hz and 20Hz stimulation conditions; coordinates in *italics* denote a voxel not part of the identified significant cluster, yet still forming the spatial centre-of-gravity (COG) of said cluster. This is increasingly possible when clusters deviate from a characteristic spheroid shape. S1 = primary somatosensory cortex; BA = Brodmann Area; SPL = superior parietal lobule; M1 = primary motor cortex; S2 = secondary somatosensory cortex; STG = superior temporal gyrus; R = right hemisphere, L = left hemisphere.

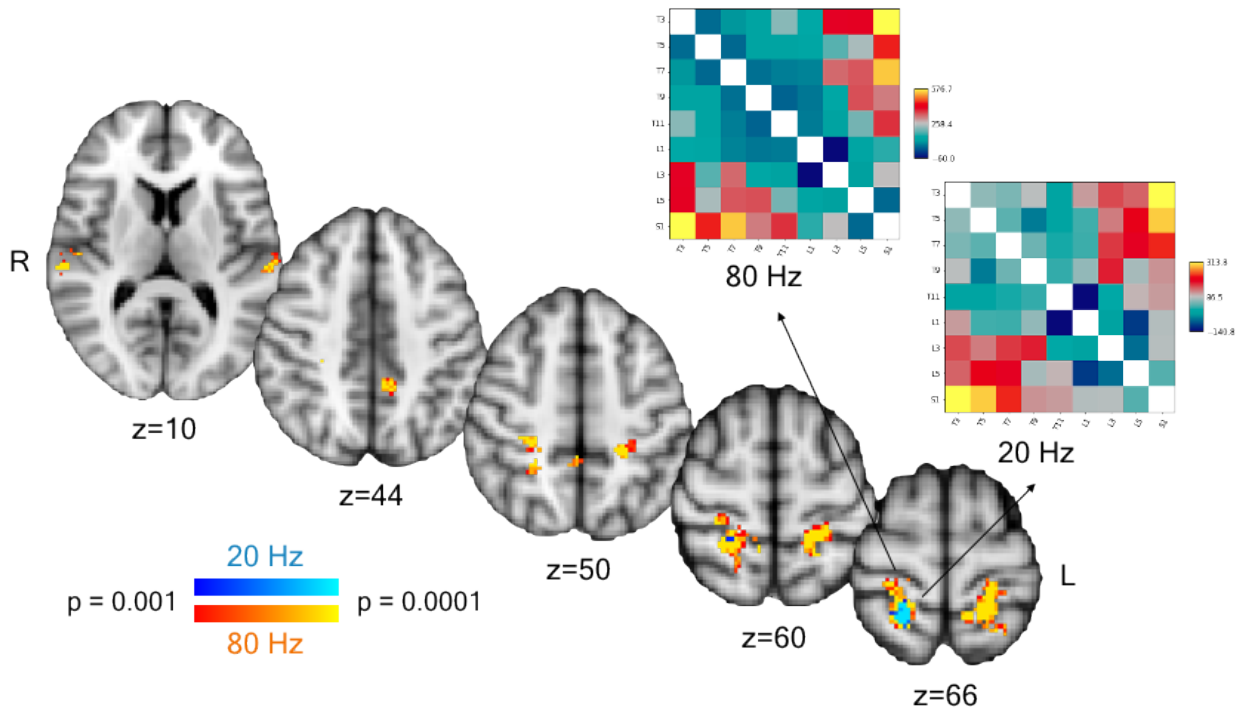

Figure 3: Brain regions identified as displaying significant representational similarity with the *segmental model* of paraspinal afferent inputs. Horizontal colour bars represent significant p-values following permutation testing for 80Hz (red-yellow) and 20Hz (blue-cyan) vibrotactile stimulation conditions. Only clusters numbering 20 or more contiguous voxels are reported. The 20Hz statistical map is presented overlaid on the 80Hz result without any reduction in the opacity of the former, as these maps are almost completely spatially overlapping. Statistical maps are overlaid on representative axial slices in the z-plane of a background image of a T1 template in MNI152 standard space. R=right hemisphere. L=left hemisphere. Arrows from the top slice point at the best group-level representational dissimilarity matrices of neural activation (brain RDMs) for 20Hz and 80Hz. Lines and columns of the brain RDMs are labelled according to the nine stimulated spinous processes $T3$-$S1$ (T=thoracic, L=lumbar, S=sacral). The vertical colour scales represent the degree of dissimilarity as quantified by the crossvalidated Mahalanobis distance.

4. Discussion

The present study set out to establish a detailed cortical mapping of the human back by assessing brain-based representations of paraspinal afferent input along the thoracolumbar axis. To this end, RSA was used to investigate the neuronal activation patterns of vibrotactile stimulation at nine different locations on the back for two specific frequencies. The frequencies were chosen to explore contributions to the activation patterns potentially resulting from different mechanoreceptors.

So far, cortical representations of the back have mainly been investigated in CLBP patients in the context of potential neural reorganization (Flor et al., 1997, Flor, 2003, Tsao et al., 2008, 2010, Hotz-Boendermaker et al., 2016). In the cases in which healthy individuals were studied, the focus was primarily oriented towards identifying cortical representations of lumbar regions with a focus on manual treatments to potentially be applied on patients (Boendermaker et al., 2014) or on specific paraspinal muscle activation (Tsao et al., 2011). However, there is a lack of detailed sensory cortical maps of the human back. To further study the pathological significance of distorted body images underlying cortical reorganization in CLBP (Lotze and Moseley, 2007), the present study specifically targeted a baseline cortical mapping of the healthy back through stimulating paraspinal afferents across the entire thoracolumbar axis.

4.1. Cortical Mapping of Paraspinal Afferent Input

In line with the hypothesis, the applied whole-brain RSA searchlight approach revealed a distinct somatotopy of the human back within S1 and S2 for bilateral vibrotactile stimulations between $T3$ and $S1$ that followed a segmental organization. This is the first time evidence for such a fine-grained cortical somatotopy of the back has been obtained, having previously only been demonstrated for other body parts such as the fingers (Besle et al., 2014, Martuzzi et al., 2014, Kolasinski et al., 2016).

In addition, the results are in line with the general observation that the spatial relationship between receptors in the body is maintained along the body-brain axis, reflected by somatotopically organized representations in the sensory homunculus (Yamada et al., 2007, Puckett et al., 2020, Schott, 1993). Furthermore, although no bilateral representations were found in M1, the extension of the model-based representational activation cluster into BA4p of the right hemisphere indicates that the central processing of paraspinal vibrotactile afferent input involves integrating contributions from somatosensory and motor cortices as previously suggested (Asanuma et al., 1980, Avanzino et al., 2014, Cole et al., 2022).

4.2. Differences between Low- and High-Frequency Stimulation

The cortical mapping obtained from correlating brain and model RDMs showed striking differences between informative activation patterns resulting from low (20Hz) compared to high frequency (80Hz) vibrotactile stimulations on the back. Bilateral 20Hz stimulation was associated only with activation patterns in one focal region of the right hemisphere, including BA2 and BA5. In contrast, 80Hz stimulation resulted in activation patterns over broader regions including BA3b and BA2, S2, BA4p and parts of the parietal cortex.

There are well known associations between vibration frequency, activated mechanoreceptors and their receptive field sizes in different S1 subregions (Avanzino et al., 2014, Weerakkody et al., 2007, Puckett et al., 2020, Iwamura et al., 1993), which could partly explain the differential results between low- (20Hz) and high-frequency (80Hz) stimulation. While the human back shows generally low tactile innervation density (Corniani and Saal, 2020), superficially located Meissner corpuscles, which preferentially get activated by low-frequency stimulations, have smaller receptive fields and their neurons are more dominant in BA2 than the neurons of deeper located Pacinian corpuscles, which are activated by high-frequency stimulations (LaMotte and Mountcastle, 1975, Talbot et al., 1968, Sherrick et al., 1990,

Iwamura et al., 1993).

However, a perfect isolated cortical read-out of the stimulated mechanoreceptor type is not realistic with the current approach. Furthermore, the applied high-frequency vibration (80Hz) might also stimulate paraspinal muscle spindle afferents. We therefore assume that the cortical response to high-frequency stimulation reflects a mixture of the different mechanoreceptor types, which might generally explain the broader activation patterns during 80Hz stimulation due to the different contributions of tactile and possibly proprioceptive afferents. Indeed, supporting the involvement of proprioceptive processing, studies investigating proprioceptive function using vibration with frequencies close to 80Hz reported activations in the motor and parietal cortices, which were also not present during pure tactile stimulation (although kinesthetic illusions were not assessed in the current study) (Romaiguère et al., 2003, Schneider et al., 2021).

4.3. Limitations

With regards to potential muscle spindle activation, it is currently not possible to say which specific muscle spindles are activated with pneuVID. The primary assumption is that superficial (longissimus and spinalis) muscles along the thoracolumbar axis are most affected in terms of activation. Inevitably, additional (rotatores and multifidi) muscles might be targeted, which show a particularly high density in muscle spindle fibres and are therefore also involved in key aspects of trunk and back proprioception (Boucher et al., 2015).

4.4. Ideas and Speculation

Altered proprioceptive inputs from paraspinal muscles might be pathophysiologically more important for the development of CLBP than, for instance, tactile sensory inputs (Beaudette et al., 2016). In order to gauge their relative importance, the topographical organization of proprioceptive afferents along the thoracolumbar

axis and their cortical targets need to be systematically investigated and differentiated. It might be worthwhile investigating whether precise anesthetization of the skin could be used to differentiate the contributions of superficial mechanoreceptors from those of more deeply located ones, as has previously been done to exclude influences of superficial afferents on observed cortical activation patterns (Goswami et al., 2011).

4.5. Outlook

Taken together, the results of the present study pave the way for a better understanding of cortical mechanisms that are involved in processing sensory input to the back. Given the demonstrated usefulness of vibrotactile stimulations to obtain a cortical somatotopy of the healthy back, in a next step a cohort of CLBP patients should be studied to investigate potential changes in the cortical representation of paraspinal afferent input and their association to clinically relevant measures, such as pain intensity and disability levels.

5. Acknowledgements

The authors wish to thank Magdalena Suter for helping with data collection and recruitment of participants.

6. Competing Interests

None of the authors have any competing interests to declare.

References

Alexandre Abraham, Fabian Pedregosa, Michael Eickenberg, Philippe Gervais, Andreas Mueller, Jean Kossaifi, Alexandre Gramfort, Bertrand Thirion, and Gaël Varoquaux. Machine learning for neuroimaging with scikit-learn. *Frontiers in neuroinformatics*, page 14, 2014.

Gunnar BJ Andersson. 8 What are the age-related changes in the spine? *Bailliere's clinical rheumatology*, 12(1):161–173, 1998.

H Asanuma, K Larsen, and H Yumiya. Peripheral input pathways to the monkey motor cortex. *Experimental brain research*, 38(3):349–355, 1980.

Laura Avanzino, Elisa Pelosin, Giovanni Abbruzzese, Michela Bassolino, Thierry Pozzo, and Marco Bove. Shaping motor cortex plasticity through proprioception. *Cerebral Cortex*, 24(10):2807–2814, 2014.

Shawn M Beaudette, Katelyn J Larson, Dennis J Larson, and Stephen HM Brown. Low back skin sensitivity has minimal impact on active lumbar spine proprioception and stability in healthy adults. *Experimental brain research*, 234(8):2215–2226, 2016.

Michel Benoist. Natural history of the aging spine. *The aging spine*, pages 4–7, 2005.

Julien Besle, Rosa-Maria Sánchez-Panchuelo, Richard Bowtell, Susan Francis, and Denis Schluppeck. Event-related fMRI at 7T reveals overlapping cortical representations for adjacent fingertips in S1 of individual subjects. *Human brain mapping*, 35(5):2027–2043, 2014.

Bart Boendermaker, Michael L Meier, Roger Luechinger, B Kim Humphreys, and Sabina Hotz-Boendermaker. The cortical and cerebellar representation of the lumbar spine. *Human brain mapping*, 35(8):3962–3971, 2014.

Jean-Alexandre Boucher, Jacques Abboud, François Nougarou, Martin C Normand, and Martin Descarreaux. The effects of vibration and muscle fatigue on trunk sensorimotor control in low back pain patients. *PloS one*, 10(8):e0135838, 2015.

Matthew Brett, Chris Markiewicz, Michael Hanke, Marc-Alexandre Côté, Ben Cipollini, Paul McCarthy, Chris Cheng, Yaroslav Halchenko, Satra Ghosh, Eric Larson, Demian Wassermann, Stephan Gerhard, and Ross Markello. NiBabel, 2022.

Luke Chang, Sam, Eshin Jolly, Jin Hyun Cheong, Anton Burnashev, Andy Chen, Marissa Clar, Seth Frey, and Paxton Fitzpatrick. NLTools, 2021.

David M Cole, Philipp Stämpfli, Robert Gandia, Louis Schibli, Sandro Gantner, Philipp Schuetz, and Michael L Meier. In the back of your mind: Cortical mapping of tactile and proprioceptive paraspinal afferent inputs. *bioRxiv*, 2022.

Giulia Corniani and Hannes P Saal. Tactile innervation densities across the whole body. *Journal of Neurophysiology*, 124(4):1229–1240, 2020.

S Darby and G Cramer. Clinical anatomy of the spine, spinal cord, and ans. *St. Louis, Mo.: Elsevier*, 2014.

Benoit P Delhaye, Katie H Long, and Sliman J Bensmaia. Neural basis of touch and proprioception in primate cortex. *Comprehensive Physiology*, 8(4):1575, 2018.

Halle R Dimsdale-Zucker and Charan Ranganath. Representational similarity analyses: a practical guide for functional MRI applications. In *Handbook of behavioral neuroscience*, volume 28, pages 509–525. Elsevier, 2018.

Halle R Dimsdale-Zucker, Maureen Ritchey, Arne D Ekstrom, Andrew P Yonelinas, and Charan Ranganath. CA1 and CA3 differentially support spontaneous retrieval of episodic contexts within human hippocampal subfields. *Nature communications*, 9(1):1–8, 2018.

Mary Beth Downs and Cindy Laporte. Conflicting dermatome maps: educational and clinical implications. *journal of orthopaedic & sports physical therapy*, 41(6): 427–434, 2011.

Naveed Ejaz, Masashi Hamada, and Jörn Diedrichsen. Hand use predicts the structure of representations in sensorimotor cortex. *Nature neuroscience*, 18(7):1034–1040, 2015.

Joset A Etzel, Jeffrey M Zacks, and Todd S Braver. Searchlight analysis: promise, pitfalls, and potential. *Neuroimage*, 78:261–269, 2013.

Stephen J Ferguson and Thomas Steffen. Biomechanics of the aging spine. *The aging spine*, pages 15–21, 2005.

Ana Ferlinc, Ester Fabiani, Tomaz Velnar, and Lidija Gradisnik. The importance and role of proprioception in the elderly: a short review. *Materia socio-medica*, 31(3):219, 2019.

C Finsback and K Mannerkorpi. Spinal and thoracic mobility-age-related reference values for healthy men and women. *Nordisk fysioterapi*, 9(3):136, 2005.

Herta Flor. Cortical reorganisation and chronic pain: implications for rehabilitation. *Journal of Rehabilitation Medicine-Supplements*, 41(41):66–72, 2003.

Herta Flor, Christoph Braun, Thomas Elbert, and Niels Birbaumer. Extensive reorganization of primary somatosensory cortex in chronic back pain patients. *Neuroscience letters*, 224(1):5–8, 1997.

Stefan Geyer, Anders Ledberg, Axel Schleicher, Shigeo Kinomura, Thorsten Schormann, Uli Bürgel, Torkel Klingberg, Jonas Larsson, Karl Zilles, and Per E Roland. Two different areas within the primary motor cortex of man. *Nature*, 382(6594): 805–807, 1996.

Stefan Geyer, Thorsten Schormann, Hartmut Mohlberg, and Karl Zilles. Areas 3a, 3b, and 1 of human primary somatosensory cortex: 2. Spatial normalization to standard anatomical space. *Neuroimage*, 11(6):684–696, 2000.

S Gilman. Joint position sense and vibration sense: anatomical organisation and assessment. *Journal of Neurology, Neurosurgery & Psychiatry*, 73(5):473–477, 2002.

J Gooijers, S Chalavi, A Roebroeck, A Kaas, and SP Swinnen. Representational similarity scores of digits in the sensorimotor cortex are associated with behavioral performance. *Cerebral Cortex*, 2022.

Ruma Goswami, Maria Fernanda Frances, and J Kevin Shoemaker. Representation of somatosensory inputs within the cortical autonomic network. *Neuroimage*, 54 (2):1211–1220, 2011.

Gregory S Harrington and J Hunter Downs III. FMRI mapping of the somatosensory cortex with vibratory stimuli: Is there a dependency on stimulus frequency? *Brain research*, 897(1-2):188–192, 2001.

Sabina Hotz-Boendermaker, Valentine L Marcar, Michael L Meier, Bart Boendermaker, and Barry K Humphreys. Reorganization in secondary somatosensory cortex in chronic low back pain patients. *Spine*, 41(11):E667–E673, 2016.

Pattariya Intolo, Stephan Milosavljevic, David G Baxter, Allan B Carman, Poonam Pal, and Joanne Munn. The effect of age on lumbar range of motion: a systematic review. *Manual therapy*, 14(6):596–604, 2009.

Yoshiaki Iwamura, Michio Tanaka, Masahiro Sakamoto, and Okihide Hikosaka. Rostrocaudal gradients in the neuronal receptive field complexity in the finger region of the alert monkey's postcentral gyrus. *Experimental Brain Research*, 92 (3):360–368, 1993.

Luke C Jenkins, Wei-Ju Chang, Valentina Buscemi, Matthew Liston, Patrick Skippen, Aidan G Cashin, James H McAuley, and Siobhan M Schabrun. Low somatosensory cortex excitability in the acute stage of low back pain causes chronic pain. *The Journal of Pain*, 23(2):289–304, 2022.

Project Jupyter. Jupyter Notebook, 2021.

Eric R Kandel, James H Schwartz, Thomas M Jessell, Steaven A Siegelbaum, and AJ Hudspeth. Principles of neural science, fifth editon. In *Principles of Neural Science*. McGraw-Hill Education, 2013.

MG Kendall. Rank correlation methods 4th edition charles griffin. *High Wycombe, Bucks*, 1970.

Hyungjun Kim, Ishtiaq Mawla, Jeungchan Lee, Jessica Gerber, Kathryn Walker, Jieun Kim, Ana Ortiz, Suk-Tak Chan, Marco L Loggia, Ajay D Wasan, et al. Reduced tactile acuity in chronic low back pain is linked with structural neuroplasticity in primary somatosensory cortex and is modulated by acupuncture therapy. *Neuroimage*, 217:116899, 2020.

Junsuk Kim, Yoon Gi Chung, Soon-Cheol Chung, Heinrich H Bülthoff, and Sung-Phil Kim. Neural categorization of vibrotactile frequency in flutter and vibration stimulations: an fMRI study. *IEEE transactions on haptics*, 9(4):455–464, 2016.

Sung Soo Kim, Manuel Gomez-Ramirez, Pramodsingh H Thakur, and Steven S Hsiao. Multimodal interactions between proprioceptive and cutaneous signals in primary somatosensory cortex. *Neuron*, 86(2):555–566, 2015.

Cathrin Koch and Frank Hänsel. Non-specific low back pain and postural control during quiet standing-a systematic review. *Frontiers in psychology*, 10:586, 2019.

James Kolasinski, Tamar R Makin, Saad Jbabdi, Stuart Clare, Charlotte J Stagg,

and Heidi Johansen-Berg. Investigating the stability of fine-grain digit somatotopy in individual human participants. *Journal of Neuroscience*, 36(4):1113–1127, 2016.

Shin-ichi Konno and Miho Sekiguchi. Association between brain and low back pain. *Journal of Orthopaedic Science*, 23(1):3–7, 2018.

Nikolaus Kriegeskorte, Rainer Goebel, and Peter Bandettini. Information-based functional brain mapping. *Proceedings of the National Academy of Sciences*, 103 (10):3863–3868, 2006.

Nikolaus Kriegeskorte, Marieke Mur, and Peter A Bandettini. Representational similarity analysis-connecting the branches of systems neuroscience. *Frontiers in systems neuroscience*, page 4, 2008a.

Nikolaus Kriegeskorte, Marieke Mur, Douglas A Ruff, Roozbeh Kiani, Jerzy Bodurka, Hossein Esteky, Keiji Tanaka, and Peter A Bandettini. Matching categorical object representations in inferior temporal cortex of man and monkey. *Neuron*, 60(6):1126–1141, 2008b.

Nikolaus Kriegeskorte, Jörn Diedrichsen, Marieke Mur, and Ian Charest. rsatoolbox, 2021.

Robert H LaMotte and Vernon B Mountcastle. Capacities of humans and monkeys to discriminate vibratory stimuli of different frequency and amplitude: a correlation between neural events and psychological measurements. *Journal of Neurophysiology*, 38(3):539–559, 1975.

Martin Lotze and G Lorimer Moseley. Role of distorted body image in pain. *Current rheumatology reports*, 9(6):488–496, 2007.

Roberto Martuzzi, Wietske van der Zwaag, Juliane Farthouat, Rolf Gruetter, and Olaf Blanke. Human finger somatotopy in areas 3b, 1, and 2: a 7T fMRI study using a natural stimulus. *Human brain mapping*, 35(1):213–226, 2014.

Wes McKinney and the Pandas Development Team. Pandas (powerful Python data analysis toolkit, 2022.

G Lorimer Moseley and Herta Flor. Targeting cortical representations in the treatment of chronic pain: a review. *Neurorehabilitation and neural repair*, 26(6): 646–652, 2012.

J Murphy, E McLoughlin, AM Davies, SL James, and R Botchu. Is T9-11 the true thoracolumbar transition zone? *Journal of Clinical Orthopaedics and Trauma*, 11 (5):891–895, 2020.

Hamed Nili, Cai Wingfield, Alexander Walther, Li Su, William Marslen-Wilson, and Nikolaus Kriegeskorte. A toolbox for representational similarity analysis. *PLoS computational biology*, 10(4):e1003553, 2014.

Michael Papadakis, Georgios Sapkas, Elias C Papadopoulos, and Pavlos Katonis. Pathophysiology and biomechanics of the aging spine. *The open orthopaedics journal*, 5:335, 2011.

Se K Park, Jung G Park, Beom S Kim, Jin D Huh, and Hee Kang. Thoracolumbar junction: morphologic characteristics, various variants and significance. *The British journal of radiology*, 89(1064):20150784, 2016.

Sabina M Pinto, Jason PY Cheung, Dino Samartzis, Jaro Karppinen, Yong-ping Zheng, Marco YC Pang, and Arnold YL Wong. Differences in proprioception between young and middle-aged adults with and without chronic low back pain. *Frontiers in Neurology*, page 1723, 2020.

Haroon Popal, Yin Wang, and Ingrid R Olson. A guide to representational similarity analysis for social neuroscience. *Social Cognitive and Affective Neuroscience*, 14 (11):1243–1253, 2019.

Uwe Proske and Simon C Gandevia. The proprioceptive senses: their roles in signaling body shape, body position and movement, and muscle force. *Physiological reviews*, 2012.

Alexander M Puckett, Saskia Bollmann, Keerat Junday, Markus Barth, and Ross Cunnington. Bayesian population receptive field modeling in human somatosensory cortex. *NeuroImage*, 208:116465, 2020.

R Rodriguez-Raecke, K Ihle, C Ritter, C Muhtz, C Otte, and A May. Neuronal differences between chronic low back pain and depression regarding long-term habituation to pain. *European Journal of Pain*, 18(5):701–711, 2014.

JP Roll and JP Vedel. Kinaesthetic role of muscle afferents in man, studied by tendon vibration and microneurography. *Experimental brain research*, 47(2):177–190, 1982.

Patricia Romaiguère, Jean-Luc Anton, Muriel Roth, Laurence Casini, and Jean-Pierre Roll. Motor and parietal cortical areas both underlie kinaesthesia. *Cognitive Brain Research*, 16(1):74–82, 2003.

Ismaila Adamu Saidu, Stanley Monday Maduagwu, Abdullahi Digil Abbas, Omotayo O Adetunji, and Abdurahman Mohammed Jajere. Lumbar spinal mobility changes among adults with advancing age. *Journal of mid-life health*, 2(2):65, 2011.

W Schellekens, M Thio, S Badde, J Winawer, N Ramsey, and N Petridou. A touch of hierarchy: population receptive fields reveal fingertip integration in Brodmann areas in human primary somatosensory cortex. *Brain Structure and Function*, 226 (7):2099–2112, 2021.

Louis Schibli, Robert Gandia, Roger Buck, Philipp Staempfli, Michael Meier, and

Philipp Schuetz. MR-safe multisegmental vibration device for cortical mapping of paraspinal afferent input. *TechRxiv*, 2021.

Christoph Schneider, Renaud Marquis, Jane Jöhr, Marina Lopes da Silva, Philippe Ryvlin, Andrea Serino, Marzia De Lucia, and Karin Diserens. Disentangling the percepts of illusory movement and sensory stimulation during tendon vibration in the EEG. *NeuroImage*, 241:118431, 2021.

Geoffrey D Schott. Penfield's homunculus: a note on cerebral cartography. *Journal of neurology, neurosurgery, and psychiatry*, 56(4):329, 1993.

Carl E Sherrick, Roger W Cholewiak, and Amy A Collins. The localization of low- and high-frequency vibrotactile stimuli. *The Journal of the Acoustical Society of America*, 88(1):169–179, 1990.

Johannes Stelzer, Yi Chen, and Robert Turner. Statistical inference and multiple testing correction in classification-based multi-voxel pattern analysis (MVPA): random permutations and cluster size control. *Neuroimage*, 65:69–82, 2013.

William H Talbot, Ian Darian-Smith, Hans H Kornhuber, and Vernon B Mountcastle. The sense of flutter-vibration: comparison of the human capacity with response patterns of mechanoreceptive afferents from the monkey hand. *Journal of neurophysiology*, 31(2):301–334, 1968.

Henry Tsao, MP Galea, and PW Hodges. Reorganization of the motor cortex is associated with postural control deficits in recurrent low back pain. *Brain*, 131 (8):2161–2171, 2008.

Henry Tsao, Mary P Galea, and Paul W Hodges. Driving plasticity in the motor cortex in recurrent low back pain. *European Journal of Pain*, 14(8):832–839, 2010.

Henry Tsao, Lieven Danneels, and Paul W Hodges. Individual fascicles of the paraspinal muscles are activated by discrete cortical networks in humans. *Clinical Neurophysiology*, 122(8):1580–1587, 2011.

Hoameng Ung, Justin E Brown, Kevin A Johnson, Jarred Younger, Julia Hush, and Sean Mackey. Multivariate classification of structural MRI data detects chronic low back pain. *Cerebral cortex*, 24(4):1037–1044, 2014.

Jaap H van Dieën, Herta Flor, and Paul W Hodges. Low-back pain patients learn to adapt motor behavior with adverse secondary consequences. *Exercise and sport sciences reviews*, 45(4):223–229, 2017.

David A Walker. JMASM9: converting Kendall's tau for correlational or meta-analytic analyses. *Journal of Modern Applied Statistical Methods*, 2(2):26, 2003.

Alexander Walther, Hamed Nili, Naveed Ejaz, Arjen Alink, Nikolaus Kriegeskorte, and Jörn Diedrichsen. Reliability of dissimilarity measures for multi-voxel pattern analysis. *Neuroimage*, 137:188–200, 2016.

Xiaosha Wang, Yangwen Xu, Yuwei Wang, Yi Zeng, Jiacai Zhang, Zhenhua Ling, and Yanchao Bi. Representational similarity analysis reveals task-dependent semantic influence of the visual word form area. *Scientific reports*, 8(1):1–10, 2018.

Michael L Waskom. Seaborn: statistical data visualization. *Journal of Open Source Software*, 6(60):3021, 2021.

Joshua A Waxenbaum, Vamsi Reddy, Caroline Williams, and Bennett Futterman. Anatomy, back, lumbar vertebrae. *StatPearls [Internet]*, 2017.

NS Weerakkody, DA Mahns, JL Taylor, and SC Gandevia. Impairment of human proprioception by high-frequency cutaneous vibration. *The Journal of physiology*, 581(3):971–980, 2007.

Kei Yamada, Yoshinari Nagakane, Kenji Yoshikawa, Osamu Kizu, Hirotoshi Ito, Takao Kubota, Kentaro Akazawa, Hiroyuki Oouchi, Shigenori Matsushima, Masanori Nakagawa, et al. Somatotopic organization of thalamocortical projection fibers as assessed with MR tractography. *Radiology*, 242(3):840–845, 2007.

Li Zhang, Lili Zhou, Qiaoyue Ren, Tahmineh Mokhtari, Li Wan, Xiaolin Zhou, and Li Hu. Evaluating cortical alterations in patients with chronic back pain using neuroimaging techniques: recent advances and perspectives. *Frontiers in Psychology*, 10:2527, 2019.